

Spectral variation in the X-ray pulsar GX 1+4 during a low-flux episode

D.K. Galloway,^{1,2} A.B. Giles,^{1,3,4} J.G. Greenhill,¹ and M.C. Storey²

¹ School of Mathematics and Physics, University of Tasmania, GPO Box 252-21, Hobart, Tasmania 7001, Australia

² Special Research Centre for Theoretical Astrophysics, School of Physics, University of Sydney, NSW, Australia, 2006

³ Laboratory for High Energy Astrophysics, Goddard Space Flight Center, Greenbelt, MD 20771, USA

⁴ Universities Space Research Association

31 July 2018

ABSTRACT

The X-ray pulsar GX 1+4 was observed with the *RXTE* satellite for a total of 51 ks between 1996 July 19 - 21. During this period the flux decreased smoothly from an initial mean level of $\approx 6 \times 10^{36} \text{ erg s}^{-1}$ to a minimum of $\approx 4 \times 10^{35} \text{ erg s}^{-1}$ (2-60 keV, assuming a source distance of 10 kpc) before partially recovering towards the initial level at the end of the observation.

BATSE pulse timing measurements indicate that a torque reversal took place approximately 10 d after this observation. Both the mean pulse profile and the photon spectrum varied significantly. The observed variation in the source may provide important clues as to the mechanism of torque reversals.

The single best-fitting spectral model was based on a component originating from thermal photons with $kT_0 \approx 1 \text{ keV}$ Comptonised by a plasma of temperature $kT \approx 7 \text{ keV}$. Both the flux modulation with phase during the brightest interval and the evolution of the mean spectra over the course of the observation are consistent with variations in this model component; with, in addition, a doubling of the column density n_H contributing to the mean spectral change.

A strong flare of duration $\lesssim 50 \text{ s}$ was observed during the interval of minimum flux, with the peak flux ≈ 20 times the mean level. Although beaming effects are likely to mask the true variation in \dot{M} thought to give rise to the flare, the timing of a modest increase in flux prior to the flare is consistent with dual episodes of accretion resulting from successive orbits of a locally dense patch of matter in the accretion disc.

Key words: binaries: symbiotic – pulsars: individual (GX 1+4) – X-rays: stars

1 INTRODUCTION

The study of X-ray pulsars has been an area of active research for almost 30 years. In spite of this there remain some significant shortfalls in the understanding of these objects. An example is the persistent pulsar GX 1+4. At the time of its discovery (Lewin, Ricker and McClintock 1971) it was one of the brightest objects in the X-ray sky. The companion to the neutron star is an M6 giant (Davidsen, Malina and Bowyer 1977). GX 1+4 is the only known X-ray pulsar in a symbiotic system. Measurements of the average spin-up rate during the 1970s gave the largest value recorded for any pulsar (or in fact any astronomical object) at ≈ 2 per cent per year. Inexplicably, the average spin-up trend reversed around 1983, switching to spin-down at approximately the same rate. Since that reversal a number of changes in the sign of the torque (as inferred from the rate of change of the pulsar spin period) have been observed (Chakrabarty et

al. 1997). Several estimates (Beurle et al. 1984, Dotani et al. 1989, Greenhill et al. 1993, Cui 1997) indicate a neutron star surface magnetic field strength of $2 - 3 \times 10^{13} \text{ G}$.

The X-ray flux from the source is extremely variable on time-scales of seconds to decades. Two principal flux states have been observed, a ‘high’ state which persisted during the spin-up period of the 1970s, and a ‘low’ state since. Although the mean flux has been increasing steadily during the current ‘low’ state it has not yet returned to the level of the 1970s. Superimposed on these long-term variations are smooth changes in the flux on time-scales of order hours to days. On the shortest time-scales the periodic variation due to the neutron star’s rotation period at around 2 min is observed.

Compared to other accretion-powered X-ray pulsars, GX 1+4 has an atypically hard spectrum extending out well past 100 keV (Frontera and Dal Fiume 1989). Historically the spectrum has been fitted with thermal bremsstrahlung

or power law models; more recent observations with improved spectral resolution generally favour a power law model with exponential cutoff. Typical values for the cutoff power law model parameters are photon index $\alpha = 1.1 - 2.5$; cutoff energy $5 - 18$ keV; e -folding energy $11 - 26$ keV. For any spectral model covering the range $1-10$ keV, it is also necessary to include a gaussian component representing iron line emission at ≈ 6.4 keV, and a term to account for the effects of photoelectric absorption by cold gas along the line of sight with hydrogen column density in the range $n_H = (4-140) \times 10^{22} \text{ cm}^{-2}$. The source spectrum and in particular the column density n_H have previously exhibited significant variability on time-scales as short as a day (Becker et al. 1976). Measurements of spectral variation with phase are few; one example of pulse-phase spectroscopy was undertaken with data from the *Ginga* satellite from 1987 and 1988 (Dotani et al. 1989). Only the column density and the iron line centre energy were allowed to vary with phase in the spectral fits, and no significant variation was observed.

The Ghosh and Lamb (1979) model predicts a correlation between torque and mass transfer rate (and hence luminosity) for accretion-driven X-ray sources. For most sources it is difficult to test such a relationship since the range of luminosities at which they are observed is limited. However the correlation between torque and luminosity has been confirmed, at least approximately, for three transient sources using data from the Burst and Transient Source Experiment (BATSE) aboard the Compton Gamma Ray Observatory (*CGRO*) and *EXOSAT* (Reynolds et al. 1996, Bildsten et al. 1997).

The situation for persistent pulsars is, however, less straightforward. The BATSE data have demonstrated that in general the torque is in fact *uncorrelated* with luminosity in these sources. The spin-up or spin-down rate can remain almost constant over intervals (referred to in this paper as a ‘constant torque state’ or just ‘torque state’) which are long compared to other characteristic time-scales of the system, even when the luminosity varies by several orders of magnitude over that time. Transitions between these states of constant torque can be abrupt, with time-scales of < 1 d when the two torque values have the same sign; alternatively when switching from spin-up to spin-down (or vice-versa) the switch generally occurs smoothly over a period of $10 - 50$ d.

It is possible that there remains some connection between the torque and luminosity, since at times the torque measured for GX 1+4 has been *anticorrelated* with luminosity (Chakrabarty et al. 1997). This behaviour has not been observed in other pulsars. One important caveat regarding the BATSE measurements is that the instrument can only measure pulsed flux. Systematic variations in pulse profiles or pulse fraction could introduce significant aliasing to the flux data, hence masking the true relationship between bolometric flux and torque. Given that pulse profile shape and torque state have shown evidence for correlation in GX 1+4 (Greenhill, Galloway and Storey 1998) this could potentially be an important effect.

In this paper we present results from spectral analysis of data obtained from GX 1+4 during 1996 using the Rossi X-ray Timing Explorer satellite (*RXTE*; Giles et al. 1995). A companion paper (Giles et al. 1999) contains detailed analysis of pulse arrival times and pulse profile changes.

2 OBSERVATIONS

The source was observed with *RXTE* between 1996 July 19 16:47 UT and 1996 July 21 02:39 UT. Several interruptions were made during that time as a consequence of previously scheduled monitoring of other sources. After screening the data to avoid periods contaminated by Earth occultations, the passage of the satellite through the South Atlantic Anomaly (SAA), and periods of unstable pointing, the total on-source duration was 51 ks. *RXTE* consists of three instruments, the proportional counter array (PCA) covering the energy range $2-60$ keV, the high-energy X-ray timing experiment (HEXTE) covering $16-250$ keV, and the all-sky monitor (ASM) which spans $2-10$ keV. Pointed observations are performed using the PCA and HEXTE instruments, while the ASM regularly scans the entire visible sky.

The background-subtracted total PCA count rate for 3 of the five proportional counter units (PCUs) comprising the PCA is shown in Fig. 1a. The other two PCUs were only active briefly at the beginning of the observation so those data are not included in the analysis. The phase-averaged PCA count rate was initially low at $\approx 80 \text{ counts s}^{-1}$. This corresponds to a flux of $\approx 6 \times 10^{36} \text{ erg s}^{-1}$ in the $2-60$ keV energy range, using the spectral model discussed in section 3 and assuming a source distance of 10 kpc. Throughout this paper we shall use this value as the source distance unless otherwise specified; the actual distance is thought to be in the range $3-15$ kpc (Chakrabarty and Roche 1997). During the course of the observation the count rate decreased to a minimum of $\approx 5 \text{ counts s}^{-1}$, corresponding to a flux of $\approx 4 \times 10^{35} \text{ erg s}^{-1}$ before partially recovering towards the end. The count rates are unusually low for this source, with other observations giving significantly higher rates; for example $\approx 320 \text{ counts s}^{-1}$ and $230 \text{ counts s}^{-1}$ (equivalent rates for 3 PCUs) in February 1996 and January 1997 respectively. At times the background-subtracted countrate during interval 2 drops significantly below zero. This is a consequence of the low source to background signal ratio (around $1:10$) during this interval coupled with statistical variations in the binned countrate values.

The observation is divided into three intervals on the basis of the mean flux (Fig. 1a). Interval 1 covers the start of the observation to just before the flux minimum. Interval 2 spans the period of minimum flux, during which time the flux was $\lesssim 30 \text{ counts s}^{-1}$ apart from ≈ 10 s during a flare (see section 5). Interval 3 covers the remaining portion of the observation, during which the mean flux increased steadily.

Accompanying the changes in flux were significant variations in pulse profile and spectral shape. Historically GX 1+4 has shown evidence of a correlation between torque state and pulse profile shape (Greenhill, Galloway and Storey 1998). Throughout the period of spin-up during the 1970s pulse profiles were typically brighter at the trailing edge with respect to the primary minimum; e.g. Doty, Hoffman and Lewin (1981). Since then, measured pulse profiles have instead usually been leading-edge bright, with less pronounced asymmetry; e.g. Greenhill et al. (1993). During interval 1 the pulse profile was observed to be leading-edge bright, similar to other observations since the 1980s. Pulsations all but ceased during interval 2, and in interval 3 the shape of the profile had changed dramatically and re-

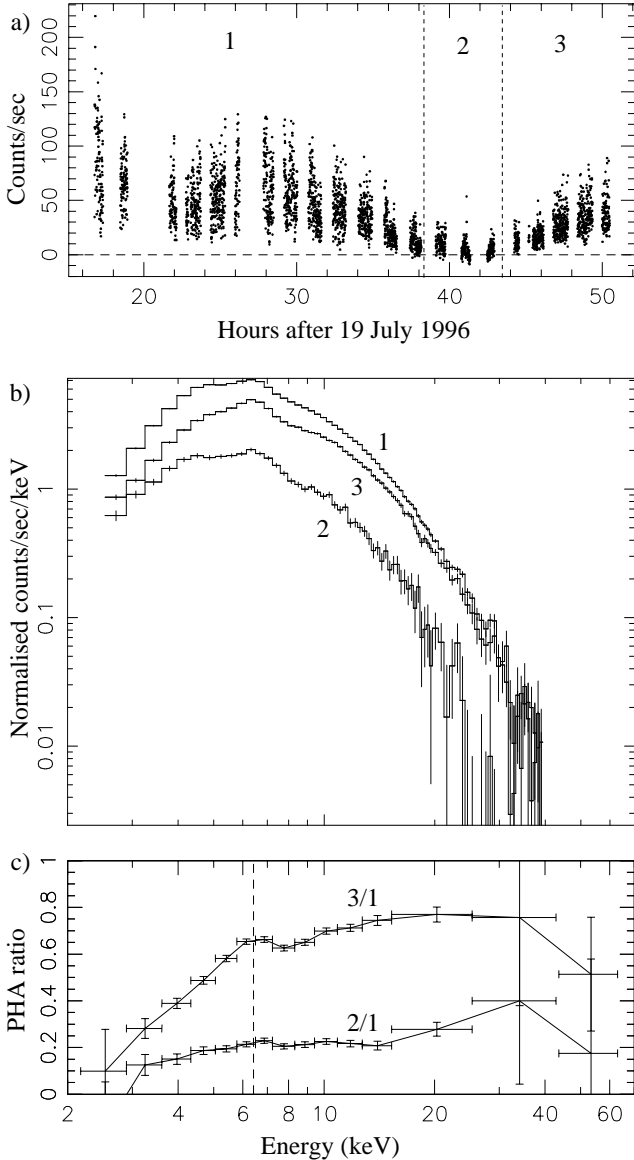


Figure 1. a) Background-subtracted PCA countrate for GX 1+4 over the course of the observation, showing the division between intervals 1, 2 and 3 (see text). The binsize is 16 s. b) Mean PCA spectra between 2.2 and 40.0 keV during each interval. The data mode used is Standard-2, with 128 channels over the total range of the instrument. c) Ratio of mean spectra in intervals 2 and 3 to that of interval 1, labelled 2/1 and 3/1 respectively. The dotted line indicates the energy of the Fe line. Spectra were obtained from the PCA except for the point covering the highest energy range, which was calculated using HEXTE data.

sembled the trailing-edge bright profiles typically observed during the 1970s (Giles et al. 1999).

The count rate spectra taken during each interval are shown in Fig. 1b. The overall spectral shape changed significantly over the course of the observation, with the spectrum becoming harder in intervals 2 and 3 compared to interval 1. The iron fluorescence line at around 6.4 keV appears more prominent in the second and third intervals. Iron line enhancement during intervals 2 and 3 is also apparent in the spectral ratios, Fig. 1c. These ratios were calculated by

subtracting the background spectrum (including a component to account for the emission from the galactic plane; see section 3) from the source spectrum for each interval and dividing the resulting spectra for intervals 2 and 3 by that of interval 1. Because the countrate drops off steeply above 10 keV the spectral bins must be made correspondingly larger to achieve a reliable ratio. The datapoint in the highest energy band for each curve was obtained from HEXTE data, while the lower energy ratios are calculated from PCA data. The decrease in flux observed from interval 1 to 2 and 3 becomes more pronounced at energies below 6 keV. Above 15 keV the spectral ratios are almost constant with energy.

3 THE SPECTRAL MODEL FITS

Instrumental background from cosmic ray interactions and as a result of passages close to the SAA are estimated using the PCABACKEST software, provided by the *RXTE* Guest Observer Facility (GOF). Due to the proximity of the source to the galactic plane, an additional component which takes into account the so-called ‘galactic ridge’ emission must be included in any spectral model. The model for this component used in our fits is identical to that fitted to survey data from this region (Valinia and Marshall 1998) with normalisations and abundance fitted to spectra taken during slews to and from the source during this observation. A secondary instrumental effect which must be taken into account to obtain the lowest possible residuals in the model fit is a consequence of the Xenon L-edge absorption feature. This feature is modelled in our spectrum by a multiplicative edge model component with energy fixed at 4.83 keV.

Candidate spectral models were tested by fitting to the count rate spectrum to minimise χ^2 using the XSPEC spectral fitting package version 10 (Arnaud 1996). In general each model takes the form of one (or more) continuum components with a gaussian component necessary to simulate the iron line emission, and a multiplicative component to account for absorption by cold matter along the line of sight. With a lower than normal count rate for the source during this observation, the primary source of error is the Poisson statistics within each energy bin rather than any instrumental uncertainty. Hence the systematic error in XSPEC was set to zero for the model fits.

Thermal bremsstrahlung and power law continuum components both resulted in formally unacceptable values of χ^2 for the interval 1 mean spectrum. Some improvement was found by fitting with various forms of power law, including a power law with exponential cutoff and a broken power law. Nevertheless, each of these models gave unacceptable values of reduced- χ^2 : 2.93 and 1.94 respectively. An acceptable fit was obtained using an analytic model based on Comptonisation of a thermal spectrum by hot plasma close to the source (*‘compTT’* in XSPEC; Titarchuk 1994), with reduced- χ^2 for the interval 1 spectra of 1.10. The Comptonisation model has thus been chosen for all spectral fitting reported in this paper. Model parameters for spectral fits from intervals 1 and 3 are shown in Table 1.

Fitting this model to the interval 2 mean spectra resulted in an acceptable χ^2_ν fit statistic of 0.7943, but with very wide confidence limits for the fit parameters. No im-

provement in the confidence intervals is obtained by freezing selected parameters to the mean values for the entire observation (e.g. T_0). The fit parameters are effectively unconstrained and as such cannot be relied upon as a measure of the source conditions. Additionally, the interval 2 spectra alone do not permit an unambiguous choice of spectral model. We cannot distinguish between cutoff powerlaw, broken powerlaw, and Comptonisation spectral models during this interval on the basis of χ^2_ν . A comparable fit can even be obtained using a model consisting of two blackbody emission components, with fitted temperatures $1.4^{1.6}_{1.2}$ keV and $6.0^{7.6}_{4.5}$ keV ($\chi^2_\nu = 0.81$; see section 5). Consequently we restrict the discussion of the mean spectral fitting results to those from intervals 1 and 3.

The Comptonisation model implementation in XSPEC offers a geometry switch which affects the fitted value of the optical depth τ_P . The switch can be set to model either disc or spherical geometries. As we will argue in section 6, neither of these are strictly appropriate for the present situation. Consequently we performed all the fitting using the disc geometry, but note that fitted values of τ_P with the spherical geometry will be approximately twice as large. The fitted values of τ_P should provide an adequate comparative measure of the degree of Comptonisation between different spectra.

The increase in line-of-sight absorption following interval 1, suggested initially by the spectral ratios (Fig. 1c), is further supported by the model fits. The fitted column density n_H more than doubles between interval 1 and 3. Spectral fits to each uninterrupted ‘burst’ of data (see Fig. 1a) indicate that the increase took place smoothly over approximately 10 hours, although significant variations in the fitted n_H values are observed on timescales as short as 2 h. *BeppoSAX* satellite observations indicate that n_H may have persisted at the level measured at the end of interval 3 at least until August 19 (Israel et al. 1998).

The input spectral temperature kT_0 is consistent with a constant value of ≈ 1 keV during the entire observation. The decrease in flux following interval 1 is associated with a marginally significant decrease in the fitted values of the scattering optical depth τ_P and the Comptonised component normalisation parameter A_C .

The model parameters associated with the gaussian component, representing fluorescence from iron in the circumstellar matter, are consistent with constant values over the course of the observation. The iron line centre energy is consistent with emission from cool matter, with no significant change in the centre energy found between intervals. The iron line equivalent width (EW) increases with marginal significance following interval 1.

4 PULSE-PHASE SPECTROSCOPY

The data from interval 1 were divided into 10 equal phase bins, and a spectrum obtained for each phase range. The ephemeris is that of Giles et al. (1999), with best-fit constant barycentre corrected period $P = 124.36568 \pm 0.00020$ s. The primary minimum is defined as phase zero. Data from interval 1 alone were used, for two reasons. Firstly, the count rate was at its highest during that time, making the signal-to-noise ratio optimal compared to the other intervals. It

was not possible to fit models reliably to pulse-phase spectra from interval 2 (due to the low count rate) or interval 3 (due to its short duration). Secondly, since the evidence of the pulse profiles suggests conditions in the source may be rather different between intervals 1, 2 and 3, this seems a better choice than simply combining all the data.

Each of the 10 spectra were then fitted with the model described in section 3. Initially, all fit parameters (barring those of the galactic ridge component) were left free to vary. Fitted values of the column density n_H , input spectrum temperature kT_0 , and the iron line component parameters were all found to be consistent with those for the mean interval 1 spectrum. Confidence limits for the scattering plasma temperature kT were very large within some phase ranges, while significant variations with phase were observed only in the normalisation parameter A_C and scattering optical depth τ_P . To improve the confidence intervals for the latter three parameters a second fit was performed with all other parameters frozen at the fitted values for the mean interval 1 spectrum. The resulting fit values are shown in Fig. 2.

Around the phase of primary minimum ($\phi = 0.0 - 0.1$) the fitted value of τ_P is significantly higher than the mean value, while kT is lower. The normalisation A_C is also significantly lower than the mean value at $\phi = 0.0$, but in the phasebin immediately following is above the confidence limits for the mean. There is little evidence for strong spectral variation from the mean at other phases, however we do note an almost monotonic decrease in the normalisation A_C from $\phi = 0.1$ and throughout the pulse cycle.

5 FLARE SPECTRA

During the period of lowest flux (interval 2) a strong flare was observed, with the peak flux rising to almost 20 times the mean level during this interval (Fig. 3a). The flare was preceded by a modest brightening of the source which began ≈ 150 s before the flare itself and lasted ≈ 60 s; a second pre-flare brightening began ≈ 50 s before the main flare, lasting ≈ 30 s. Both the flare and the pre-flare activity occurred within the extent of two pulse periods. From the ephemeris determined for the full data set (Giles et al. 1999), a primary minimum would have occurred between the first and second pre-flares had the source been pulsing as was observed during intervals 1 and 3. The instantaneous flux during the flare peaked at $\approx 105 \text{ count s}^{-1}$, compared to the mean rate during interval 2 of $\approx 5 \text{ count s}^{-1}$. No comparable events occurred at other times during interval 2. During intervals 1 and 3, the significant variations between successive pulse profiles make it difficult to rule out flares with peaks having similar heights above the mean level. Certainly no flares with the same proportional increase in flux compared to the mean occurred over the course of the observation.

The count rate during this interval was too low to obtain useful full-resolution spectra. Instead, low-resolution spectra at various times were extracted from the uninterrupted portion of data within which the flare was observed. The PHA ratios obtained by dividing the various spectra are shown in Fig. 3b. The top panel shows the ratio of the mean spectrum following the flare to that preceding it (excluding the flare itself). Mean flux decreased by around 50 per cent following the flare, with no strong evidence of spectral variation. The

Table 1. Fit parameters for intervals 1 and 3 using the best-fitting model based on Comptonisation of soft photons by hot plasma. kT_0 is the temperature of the thermal input spectrum, kT and τ_P are the temperature and optical depth respectively of the scattering plasma, and A_C is the normalisation parameter for the Comptonised model component. The model also incorporates a gaussian component representing iron line emission, with E_{Fe} the line centre energy, σ the line width, A_{Fe} the normalisation and EW the equivalent width. Both these components are attenuated by photoelectric absorption by cold matter along the line of sight, with column density n_H . Data used is from PCA mode Standard-2. Confidence intervals are 90 per cent; fit statistic is reduced- χ^2 (χ^2_ν).

Parameter	Interval 1	Interval 3
n_H ($\times 10^{22} \text{ cm}^{-2}$)	$13.6^{14.4}_{12.9}$	$28.8^{32.3}_{25.0}$
kT_0 (keV)	$1.18^{1.21}_{1.15}$	$1.00^{1.13}_{0.88}$
kT (keV)	$7.77^{8.53}_{7.19}$	$8.61^{14.1}_{6.93}$
τ_P	$3.26^{3.48}_{3.02}$	$2.90^{3.51}_{1.97}$
A_C (photons $\text{cm}^{-2} \text{ s}^{-1} \text{ keV}^{-1}$)	$(5.11^{5.56}_{4.64}) \times 10^{-3}$	$(4.42^{4.98}_{3.51}) \times 10^{-3}$
E_{Fe} (keV)	$6.406^{6.450}_{6.357}$	$6.37^{6.46}_{6.20}$
σ	$0.32^{0.400}_{0.23}$	$0.37^{0.59}_{0.20}$
A_{Fe} (photons $\text{cm}^{-2} \text{ s}^{-1} \text{ keV}^{-1}$)	$(4.234^{93}_{3.74}) \times 10^{-4}$	$(5.0^{8.3}_{3.8}) \times 10^{-4}$
EW (keV)	$0.18^{0.21}_{0.16}$	$0.24^{0.36}_{0.19}$
χ^2_ν	1.105 (64 d.o.f)	0.7251 (64 d.o.f)

second and third plots show the ratios of the pre-flare (interval A on Fig. 3a) and flare (intervals B and C) spectra vs. the mean (excluding the flare). In each case there is no evidence of spectral variation; each ratio is consistent with constant PHA ratio in the range 3-20keV. The pre-flare exhibits only a modest increase in flux of around 50 per cent, while during the 58 s window encompassing the flare itself the mean flux increased by 4-5 times.

The bottom panel shows the PHA ratio between the falling and rising parts of the main flare (intervals C and B respectively). The ratio is constant barring a broad dip between 6 and 12 keV. Examination of the spectra indicate that this dip is not due to any global change in the spectral shape, but rather a localised decrease in flux within that energy range as the flare developed. Modelling the spectra from the rising and falling parts using the two-temperature model described in section 3, we find that the variation can be fitted best by a decrease in the temperature of the cooler component ($\chi^2_\nu = 1.6$) although the change in temperature is not statistically significant.

6 DISCUSSION

Re-analysed BATSE data confirm that GX 1+4 underwent a torque reversal from spin-down to spin-up around 1996 August 2, approximately 10 days after the RXTE observation (Giles et al. 1999). Since contributions to the net torque on the neutron star may come from both accreted material and magnetic stresses within the disc, it seems reasonable to suggest that changes in the magnetosphere or disc structure which cause the torque reversal may occur some time before a measurable effect is seen on the star itself. We therefore suggest that the spectral and pulse profile changes measured during our observation are related to the (presently unknown) phenomenon which causes torque reversals. Additional support for this connection is provided

by the observation of dramatic pulse profile shape changes during the *RXTE* observation coupled with the previously noted correlation between pulse profile shape and torque state (Greenhill, Galloway and Storey 1998). Until an observation can be made which encompasses the precise time a torque reversal is occurring it may be impossible to determine more about the process.

Comptonisation models have been used to fit spectra for this source from past observations, e.g. Staubert et al. (1995); however it has not previously been possible to eliminate all other candidate models on the basis of the χ^2 fit parameter. The particular model used for the spectral fitting simulates Comptonisation in an unmagnetised plasma (Titarchuk 1994), and since the available evidence points towards a strong magnetic field in GX 1+4 (although this awaits confirmation by more direct measurements such as a cyclotron resonance line) the model fit parameters may not be an accurate measure of the source conditions. It is likely that the principal effect of the magnetic field will be to make the spectral parameters dependent on the emission angle. Hence the model fit parameters obtained from the mean spectra are expected to be a reasonable approximation of the actual values (L. Titarchuk, pers. comm.)

Assuming that the majority of the X-ray emission originates from a blackbody at most the size of the neutron star ($R_* \approx 10 \text{ km}$), we expect a temperature $kT_0 \gtrsim 0.5 \text{ keV}$. The temperature of the input spectrum $kT_0 \approx 1 \text{ keV}$ obtained from the model fits is consistent with this calculation. Rough estimates of the accretion column density can be made based on the mass transfer rate derived from the luminosity, and assuming a simple column geometry. The accretion luminosity $L_{acc} \approx GM_*\dot{M}/R_*$ and hence during interval 1 $\dot{M} \approx 2 \times 10^{16} \text{ g s}^{-1}$. Assuming that the accretion column radius R_c is some fraction f of the neutron star radius R_* , and the column plasma is moving at approximately the free fall velocity $\approx 0.5c$, the estimated optical depth for Thompson scattering is $\approx 0.17/f$. In general f

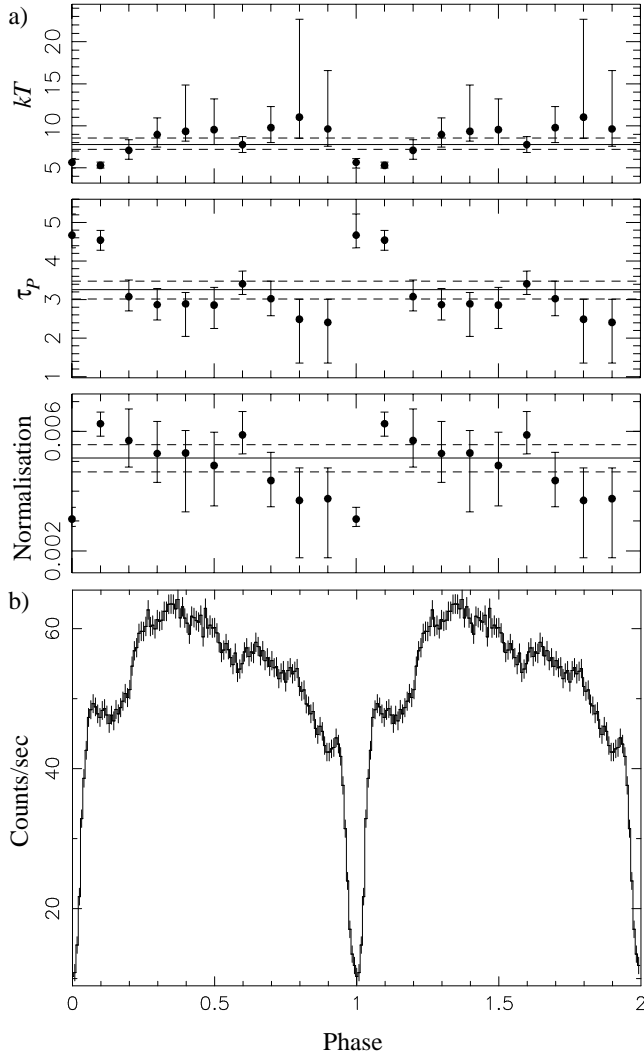


Figure 2. a) Spectral model fit parameters with pulse phase during interval 1. The top panel shows the scattering plasma temperature kT ; the middle panel the optical depth for scattering τ_P ; while the bottom panel shows the model component normalisation A_C . The errorbars show the 90 per cent confidence limits. The fitted parameter values for the mean interval 1 spectra are shown by the solid lines; 90 per cent confidence intervals as dotted lines. b) Pulse profile from background-subtracted Event-mode PCA data. Two full pulse periods are shown for clarity.

is subject to considerable uncertainties particularly given the over-simplistic geometry adopted here, but we estimate $f \approx 4 \times 10^{-2}$ (e.g. Frank, King and Raine 1992) and thus the optical depth $\tau \approx 5$, close to the model fit values.

The pulse phase spectroscopy results also show that τ_P , kT and A_C are significantly modulated at the pulsar rotation period. Consequently we propose that the Comptonisation model provides a realistic picture of spectral formation in this source, with scattering taking place in the accretion column. Thus the kT parameter can be interpreted as the mean temperature of the accretion column plasma over the region in the column where scattering takes place. The model normalisation parameter A_C is somewhat more difficult to relate to a physically measurable quantity, since

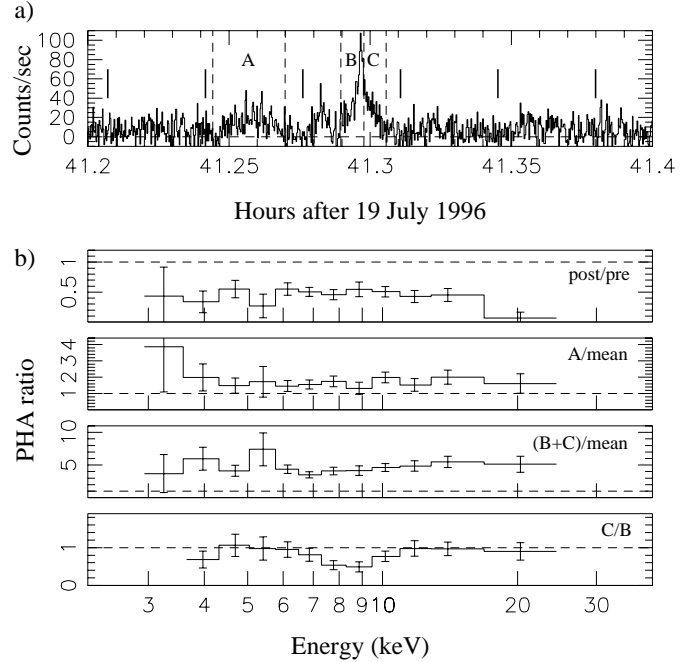


Figure 3. a) Event-mode PCA lightcurve (averaged over 1 s bins) during interval 2 showing the flare. Thick lines show the predicted times of primary minima from the ephemeris of Giles et al. (1999). The three intervals of interest are labelled A, B and C, for the pre-flare brightening, flare rise, and flare fall respectively. b) The top panel shows the ratio of the mean post-flare to the mean pre-flare spectrum (excluding the flare itself). The second panel shows the ratio of the spectrum during the pre-flare increase (interval A in Fig. 3a) to the mean spectrum (excluding the flare). The third panel shows the ratio of the flare spectra (intervals B and C) to the mean (excluding the flare). The fourth panel shows the ratio of the spectrum during the flare decrease (C) to that during the flare increase (B).

both the kT and τ_P parameters can also affect the total flux from the model component.

The spectral ratios (Fig. 1c) and the spectral fit parameters strongly suggest that the variations in the mean spectra during the course of the observation are due to two factors. The decrease in flux which is essentially independent of energy is presumably a result of decreased rate of mass transfer to the neutron star \dot{M} . This is accompanied by a strong increase in absorption by cold material causing the flux decrease below 6 keV.

Variations in the column density n_H on time-scales of ≈ 2 h have not previously been observed in this source. The iron line energy and the relationship between equivalent width and n_H are consistent with the spherical distribution of matter suggested by Kotani et al. (1999), however the variation is much too rapid to be attributable to the negative feedback effect which those authors suggest regulates mass transfer to the neutron star in the long term. The rapid variation may be an indication of significant inhomogeneities in the circumstellar matter, or alternatively that the giant wind velocity is much faster than 10 km s^{-1} as suggested by infrared observations of the companion (Chakrabarty et al. 1998).

Variation in the spectral fit parameters with pulse phase

may provide clues to the distribution of matter in the accretion column. The sharp dip in the pulse profiles is associated with a significant increase in the scattering optical depth τ_P and decrease in the Comptonisation component normalisation parameter A_C (Fig. 2). Such an effect may be observed if the accretion column is viewed almost directly along the magnetic axis, resulting in a much greater path length for photons propagating through the relatively dense matter of the column; essentially an ‘eclipse’ of the neutron star pole by the accretion column. Preliminary Monte Carlo modelling based on Comptonisation as the source of high-energy photons supports this as a possible mechanism (Galloway, 1999, work in progress). Accretion column eclipses have previously been postulated to explain dips in pulse profiles from A 0535+262 (Cemeljic and Bulik 1998) and RX J0812.4-3114 (Reig and Roche 1999). That the plasma temperature kT is also low around the phase of primary minimum may be related to the bulk motion of the column plasma, since the relative velocity of the plasma in the observer’s frame will depend on orientation (and hence pulse phase). The velocity of bulk motion is likely to be many orders of magnitude above the thermal velocity (in the plasma rest frame) and so may result in observable variation of this fit parameter with pulse phase. The asymmetry of the normalisation A_C with respect to the primary minimum furthermore points to significant asymmetry of the emission on the ‘leading’ and ‘trailing’ side of the pole. Such asymmetry may originate from a nonzero relative velocity between the disc and column plasma where the disc plasma becomes bound to the magnetic field lines and enters the magnetosphere (Wang and Welter 1981). The additional observation that the width of the dip decreases with increasing energy may point towards a role for resonant absorption (Giles et al. 1999).

The observation of a short-duration flare during the minimum flux period provides a further example of previously unseen behaviour in this source. With the peak flux during the flare rising to almost 20 times the mean level, and with no other comparable events observed during interval 2, it is likely that the flare was due to a short-lived episode of enhanced accretion. The mean accretion rate during interval 2 can be estimated to be $\approx 2.5 \times 10^{15} \text{ g s}^{-1}$ (Frank, King and Raine 1992); the increased luminosity observed during the flare thus implies additional accretion of at least $5 \times 10^{17} \text{ g}$. In order to measure the instantaneous \dot{M} throughout the flare it would be necessary to correct for the effects of anisotropic emission from the neutron star surface as well as changing observation angle with the star’s rotation. Since the geometry is essentially unknown, and beam patterns rather model dependent, this is not yet possible.

We do however note that the delay between the start of the pre-flare increase (‘A’ in Fig. 3) and the flare itself is $\approx 150 \text{ s}$. The relative angular velocities of the disc plasma and the neutron star magnetic field lines at the inner disc radius imply a periodicity significantly different from that resulting from the neutron star’s rotation. From the mean interval 2 luminosity and the estimated surface magnetic field strength for GX 1+4 of $3 \times 10^{13} \text{ G}$ we estimate the inner disc radius as $2.7 \times 10^7 \text{ m}$. A locally dense patch of plasma rotating with Keplerian velocity in the disc would pass close to the region where plasma enters the accretion column originating from each pole every 150 s or so. Thus it is conceivable that these

two events represent successive passages of the same patch through the column uptake zone in the disc. After the second passage, the patch is presumably completely transmitted to the star and so no further flaring behaviour is seen.

If \dot{M} variations are a significant factor in the evolution of the flare, we might see other indications in the flare shape. If the polar region cools much more slowly than the flare timescale an asymmetric flare might be observed. Spectral model fits might also indicate cooling of the emission component originating from the pole. However, the flare appears almost completely symmetric, and spectral fits to the rising and falling parts of the flare do not exhibit cooling at any statistically significant level.

ACKNOWLEDGMENTS

We would like to thank Dr. K. Wu for many helpful discussions and suggestions during the preparation of this paper. The *RXTE* GOF provided timely and vital help and information, as well as the archival observations from 1996 and 1997. We would also like to thank the BATSE pulsar group for providing the timing data.

REFERENCES

- Arnaud K.A., 1996, in Jacoby G.H., Barnes J., eds, *Astronomical Data Analysis Software and Systems V*, A.S.P. Conference Series Vol. 101, p. 17.
- Becker R.H., Boldt E.A., Holt S.S., Pravdo S.H., Rothschild R.E., Serlemitsos P.J., Swank J.H., 1976, *ApJ*, 207, L167
- Beurle K., Bewick A., Harper P.K.S., Quenby J.J., Spooner N.J.C., Fenton A.G., Fenton K.B., Giles A.B., Greenhill J.G., Warren D.M., 1984, *AdSpR*, 3(10-12), 43
- Bildsten L., Chakrabarty D., Chiu J., Finger M.H., Koh D.T., Nelson R.W., Prince T.A., Rubin B.C., Scott D.M., Stollberg M., Vaughan B.A., Wilson C.A., Wilson R.B., 1997, *ApJS*, 113, 367
- Cemeljic, M., Bulik, T., 1998, *AcA*, 48, 65
- Chakrabarty D., Roche P., 1997, *ApJ*, 489, 254
- Chakrabarty D., Bildsten L., Finger M.H., Grunsfeld J.M., Koh D.T., Nelson R.W., Prince T.A., Vaughan B.A., Wilson R.B., 1997, *ApJ*, 481, L101
- Chakrabarty D., van Kerkwijk M.H., Larkin J.E., 1998, *ApJ*, 497, L39
- Cui W., 1997, *ApJ*, 482, L163
- Davidson A., Malina R., Bowyer S., 1977, *ApJ*, 211, 866
- Dotani T., Kii T., Nagase F., Makishima K., Ohashi T., Sakao T., Koyama K., Tuohy I.R., 1989, *PASJ*, 41, 427
- Doty J.P., Hoffman J.A., Lewin W.H.G., 1981, *ApJ*, 243, 257
- Frank J., King A., Raine D., 1992, *Accretion Power in Astrophysics*, 2nd edn. Cambridge Univ. Press, Cambridge.
- Frontera F., Dal Fiume D., 1989, in Hunt J., Battrick B., eds, *Proc. 23rd ESLAB Symposium on Two Topics in X-ray Astronomy 1. X-ray Binaries*. ESA, Paris, p. 57
- Ghosh P., Lamb F.K., 1979, *ApJ*, 234, 296
- Giles A.B., Jahoda K., Swank J.H., Zhang W., 1995, *PASA*, 12, 219
- Giles A.B., Greenhill J.G., Galloway D.K., Storey M.C., 1999, submitted to *ApJ*
- Greenhill J.G., Sharma D.P., Dieters S.W.B., Sood R.K., Waldron L., Storey M.C., 1993, *MNRAS*, 260, 21
- Greenhill J.G., Galloway D.K., Storey M.C., 1998, *PASA*, 15, 254
- Israel G.L., Angelini L., Burderi L., Campana S., Dal Fiume D.,

- Frontera F., Mereghetti S., Orlandini M., van Paradijs J., Parmar A.N., Piraino S., Ricci D., Santangelo A., Stella L., Vietri M., White N.E., 1998, in Scarsi L., Bradt H., Giommi P., Fiora F., eds., *The Active X-ray Sky: Results from BeppoSAX and RXTE*. Elsevier, Amsterdam, p.141
- Kotani T., Dotani T., Nagase F., Greenhill J.G., Pravdo S.H., Angelini L., 1999, *ApJ*, 510, 369
- Lewin W.H.G., Ricker G.R., McClintock J.E., 1971, *ApJ*, 169, L17
- Reig P., Roche P., 1999, *MNRAS*, 306, 95
- Reynolds A.P., Parmar A.N., Stollberg M.T., Verbunt F., Roche P., Wilson R.B., Finger M.H., 1996, *A&A*, 312, 872
- Staubert R., Maisack M., Kendziorra E., Draxler T., Finger M.H., Fishman G.J., Strickman M.S., Starr C.H., 1995, *AdSpR*, 15, 5119
- Titarchuk L. 1994, *ApJ*, 434, 570
- Valinia A., Marshall F.E., 1998, *ApJ*, 505, 134
- Wang Y.M., Welter G.L., 1981, *A&A*, 102, 97